BRANCHLINE-COUPLERS WITH IMPROVED DESIGN FLEXIBILITY AND BROAD BANDWIDTH

Bernd Mayer and Reinhard Knöchel

Technische Universität Hamburg-Harburg
Arbeitsbereich Hochfrequenztechnik
Postfach 90 14 03, D-2100 Hamburg 90
West Germany

Abstract
Analytical formulas are derived, which allow to fully exploit the design flexibility inherent in two-arm branchline-couplers with open stubs at the symmetry-planes in order to avoid low-impedance lines. A broadbanding procedure is given also, which for example improves the operating-bandwidth of a two-arm coupler up to 40% while maintaining very flat coupling characteristics.

Introduction

Symmetrical branchline directional couplers with two or more branches and a power-split of 3dB find many applications in practical systems. They offer the advantages of combining forward (codirectional) coupling characteristics with structural simplicity, thus avoiding narrow line gaps or the need for bond-wires, as is required for other types of couplers built with microstrip techniques.

On the other hand, two disadvantages arise:
- inconvenient line impedances,
- narrow operating bandwidth.

Analysis of two branch couplers

A non-impedance transforming branchline-coupler has a two-fold symmetry about the F_1 and F_2 planes, as shown in Fig. 1. The conventional design for a 3dB-coupler requires $\theta_1 = \theta_2 = 45°$, $Z_1 = Z_0/\sqrt{2}$ and $Z_2 = Z_0$.

The two-fold symmetry can be utilized to analyze the structure in terms of eigenreflections /1/.

Designing a branchline-coupler means synthesizing the eigenreflections by choosing Z_1, θ_1, Z_2 and θ_2. It is clear, that the structure of Fig. 1 offers only a limited degree of freedom. A more flexible design is possible with the circuit of Fig. 2, /2/ /3/ where additional open stubs are connected at the planes F_1 and F_2.

Eigenreflections are related to eigenadmittances via the relationship

$$jB_{(e,o)} = \frac{1 - s_{(e,o)}}{1 + s_{(e,o)}} \quad , \qquad \begin{matrix} e = \text{even-mode excitation} \\ o = \text{odd-mode excitation} \end{matrix} \qquad (1)$$

where characteristic impedances are normalized to the port impedance Z_0. Defining

$$t_j = \tan \theta_j \quad , \qquad j = 1, 2, 3, 4 \qquad (2)$$

the eigenadmittances can be written down as

$$B_{ee} = \frac{t_1}{Z_1} R_1 + \frac{t_2}{Z_2} R_2 \qquad B_{oe} = \frac{t_1}{Z_1} \cdot R_1 + \frac{1}{t_2 Z_2}$$
$$B_{eo} = \frac{1}{t_1 Z_1} + \frac{t_2}{Z_2} R_2 \qquad B_{oo} = -\frac{1}{t_1 Z_1} - \frac{1}{t_2 Z_2} \quad , \qquad (3)$$

where the abbreviations

$$R_1 = \frac{\frac{Z_1}{t_1} + \frac{Z_3}{t_3}}{\frac{Z_3}{t_3} - Z_1 t_1} \qquad R_2 = \frac{\frac{Z_2}{t_2} + \frac{Z_4}{t_4}}{\frac{Z_4}{t_4} - Z_2 t_2} \qquad (4)$$

are introduced. One of the equations (3) depends on the others.

Fixing five of the eight variables in (3) (within limits) allows the calculation of the remaining quantities. If, for instance, all the characteristic impedances are fixed, one line length, say t_3, can be chosen additionally. Then we can resolve (3) for the remaining line lengths. This yields

$$t_1 = \frac{1}{2} \frac{Z_1 \Delta B}{1 + \frac{Z_1^2}{Z_3} \Delta B \, t_3} \left\{ 1 \pm \sqrt{1 - \frac{1 + \frac{Z_1^2}{Z_3} \Delta B \, t_3}{\frac{1}{4} Z_1^2 \Delta B^2}} \right\} \qquad (5a)$$

$$t_2 = -\frac{1}{Z_2 \left(B_{oo} + \frac{1}{Z_1 t_1} \right)} \qquad \Delta B = (B_{oe} - B_{oo}) \qquad (5b)$$

$$t_4 = \frac{\left(\frac{1}{Z_1 t_1} + B_{eo} \right) \left(\frac{1}{Z_1 t_1} + B_{oo} \right) + \frac{1}{Z_2^2}}{B_{oo} - B_{eo}} Z_4 \quad . \qquad (5c)$$

Obviously (5) leads to two possible solutions for t_1 when t_3 is fixed. The length t_3 has to fulfill the condition

$$t_3 \leq \frac{\frac{1}{4} Z_1^2 (B_{oe} - B_{oo})^2 - 1}{\frac{Z_1^2}{Z_3} (B_{oe} - B_{oo})} \quad . \qquad (6)$$

As an example all the characteristic impedances are set to 70Ω. The eigenreflections were chosen under an angle of 45° with respect to the real axis. One obtains from (1) $B_{ee} = 1+\sqrt{2}$, $B_{eo} = 1-\sqrt{2}$, $B_{oe} = -1+\sqrt{2}$, $B_{oo} = -1+\sqrt{2}$. The two solutions for a choice of $\theta_3 = 50°$ are shown in Fig. 3 and Fig. 4. In Fig.

CH2848-0/90/0000-0391$01.00 © 1990 IEEE

5 a solution is shown, when θ_3 is chosen such that (6) is an equality. As can clearly be seen that solution shows the best frequency behaviour of the eigenvalues. If $t_3 = t_4 = 0$ i.e. no stubs are used, four variables disappear and only one can still be chosen, for example Z_1. Nevertheless solutions of (5) other than the conventional one remain.

Broadbanding branchline couplers

Because even the conventional branchline couplers suffer from a too narrow bandwith for many applications, it is important to find some realizable circuits in order to increase the operating frequency range. Some work was done on broadbanding hybrid couplers in the past /4-7/. Based on that work, a novel broadbanding procedure will be developed in the following for the coupler structure shown in Fig. 1 with $\theta_1 = \theta_2 = 45°$. Since the input impedance of the coupler is real at the center frequency f_o, the reflection coefficient $S_{11}(f_o)$ is real also. For a defined mismatch at the center frequency the corresponding input impedance Z_I can be calculated.

$$Z_I/Z_o = (1 + S_{11}(f_o))/(1 - S_{11}(f_o)) \qquad (7)$$

Now we can calculate the impedance level of the "inner" coupler, i.e. the characteristic impedances Z_1 and Z_2.

$$\frac{Z_2}{Z_o} = \sqrt{\frac{-3}{2}\left(1 - \frac{Z_I}{Z_o}\right) + \sqrt{\frac{9}{4}\left(1 - \frac{Z_I}{Z_o}\right)^2 + \frac{Z_I}{Z_o}}} \qquad (8)$$

$$Z_1/Z_o = Z_2/(Z_o \cdot \sqrt{2}) \qquad (9)$$

As proposed in /7/, a single $\lambda/2$-section with characteristic impedance Z_c is added in series to the coupler inputs. If Z_c is increased to values greater than 50Ω, a minimum appears in the return loss characteristics at band center, leading to two attenuation maxima when the frequency deviates. Z_c is chosen such that the previously defined value of $|S_{11}|$ re-appears at a maximum frequency deviation $\pm B/2$, i.e. $|S_{11}|$ is lower than the prescribed value inside this frequency range. Because this procedure leads not to two perfectly matched points as in /7/ one gets an improved solution. Moreover, it is possible to widen the bandwidth by cascading more $\lambda/2$-length lines to the ports. The results of a broadbanded coupler with two $\lambda/2$-length lines in cascade at each port are shown in Fig. 6. Alternatively, it is possible to get almost the same features by adding a $\lambda/2$-length open stub or a $3\lambda/4$-length short stub in parallel to one series branch as shown in Fig. 7. Now it is straightforward to combine the two methods to get a broader and broader bandwidth. The couplers shown in Fig. 6 and Fig. 7 were computer optimized. Fig. 8 shows results based on the coupler of Fig. 5, broadbanded with single $\lambda/2$-length sections, in order to demonstrate that the procedure works also for couplers like that shown in Fig. 2.

Experimental results

To verify the theoretical work, various 3dB couplers were built. Two examples are given for two-arm couplers:

(i) a hybrid coupler with two series $\lambda/2$-length branches in cascade (Fig. 9),

(ii) a hybrid coupler with one series $\lambda/2$-length branch and one $\lambda/2$-length open stub in parallel (Fig. 10)

The couplers were built with microstrip-techniques, using a teflon substrate with $\varepsilon_r = 2{,}2$ and $h = 0{,}254$ mm.

Conclusions

The presented analysis shows, that it is an easy task to avoid low-impedance lines in the design of two-arm branchline couplers. Two possibilities are outlined:

- to use the conventional coupler topology and deviate from the traditional choice of line lengths and characteristic impedances.
- to add open stubs at the symmetry-planes of the coupler, as proposed in /2/.

Other possibilities are

- splitting a low-impedance line into two lines with higher impedance in parallel. The width of the two lines can be much less, compared to the low-impedance line, whereas the effective admittance at the branching-junctions is the same,
- yet another open stub can be connected at the branching-junctions. This stub is active for even- and odd-excitations. Hence all eigenvalues can be set by adjusting the lengths of open lines.

However, all deviations from the conventional design of a branchline coupler (concerning the "internal" design) lead to a decrease in coupler bandwidth and symmetry with respect to center frequency. Therefore, in the second part of the paper, a method is described, how the operating bandwidth of a branchline coupler can be increased very efficiently: Cascading $\lambda/2$-length transmission-lines and open stubs is very well suited for broadbanding conventional and other branchline couplers. The bandwidth of a two-arm coupler can be increased from 10% to a relative bandwidth of more than 40% while maintaining very flat amplitude characteristics.

References

/1/ Montgomery, C.G., Dicke, R.H. and Purcell, E.M.: Principles of microwave circuits. Mc Graw Hill, 1948.

/2/ Ashoka, H.: New type of branch-line hybrids. 18th European Microwave Conference, Stockholm 1988, pp. 785-790.

/3/ Khilla, A.M.: Tunable branch-line hybrids. Frequenz, vol. 43, 1989, pp. 194-200.

/4/ Riblet, G.P.: A directional coupler with very flat coupling: IEEE Trans. MTT, vol. MTT-26, 1978, pp. 70-74.

/5/ Okoshi, T., Imai, T., Ito, K.: Computer-oriented synthesis of optimum circuit pattern of 3-dB hybrid ring by the planar circuit approach. IEEE Trans. MTT, vol. MTT-29, 1981, pp. 194-202.

/6/ Wright, A.S., Judah, S.K.: Very broadband flat coupling hybrid ring. El. Lett., vol. 23, 1987, pp. 47-49.

/7/ Ashforth, J.V.: Design equations to realise a broadband hybrid ring or a two-branch guide coupler of any coupling coefficient. El. Lett., vol. 24, 1988, pp. 1276-1277.

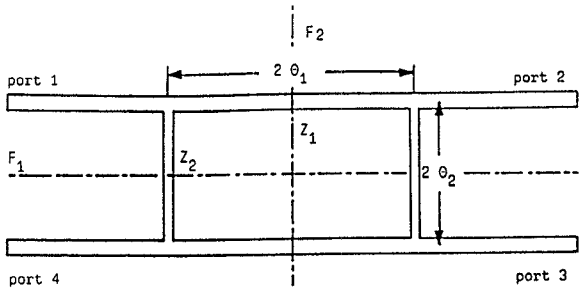

Fig. 1. Two branch coupler with two-fold symmetry (θ_i = line lengths, Z_i = characteristic impedances)

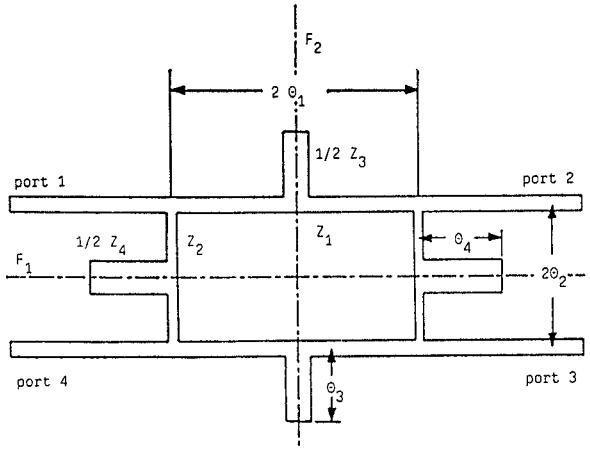

Fig. 2. Extended two branch coupler with open stubs at the symmetry-planes

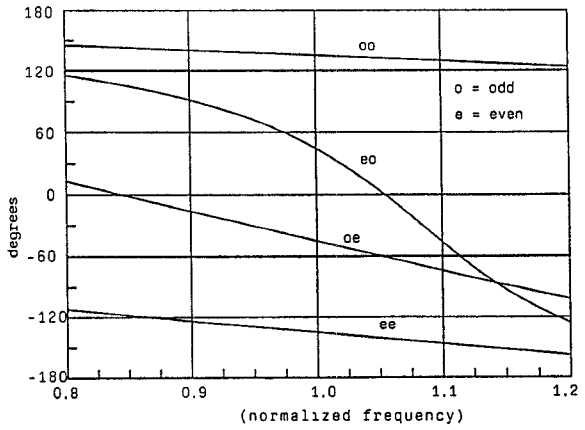

Fig. 3. Frequency behaviour of the eigenvalues of a coupler pictured in Fig. 2. All characteristic impedances are set to 70.7Ω. θ_3 is set to 50.0° electrical length. The calculations yield θ_1 = 19.7°, θ_2 = 57.9° and θ_4 = 15.2° electrical length.

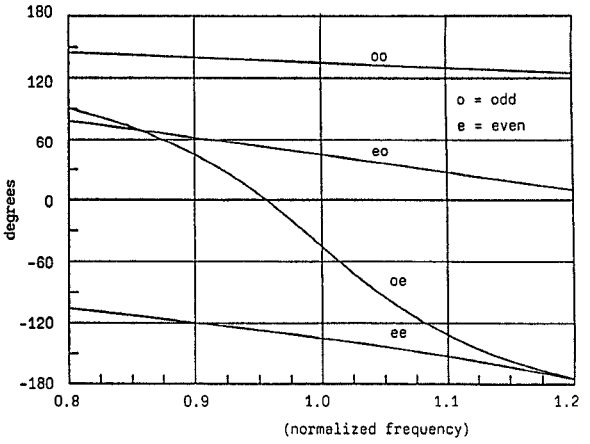

Fig. 4. Frequency behaviour of the eigenvalues of a coupler pictured in Fig. 2. All characteristic impedances are set to 70.7Ω. θ_3 is set to 50.0° electrical length like in Fig. 3. The calculations yield a second solution of θ_1 = 39.5°, θ_2 = 24.5° and θ_4 = 15.2° electrical length.

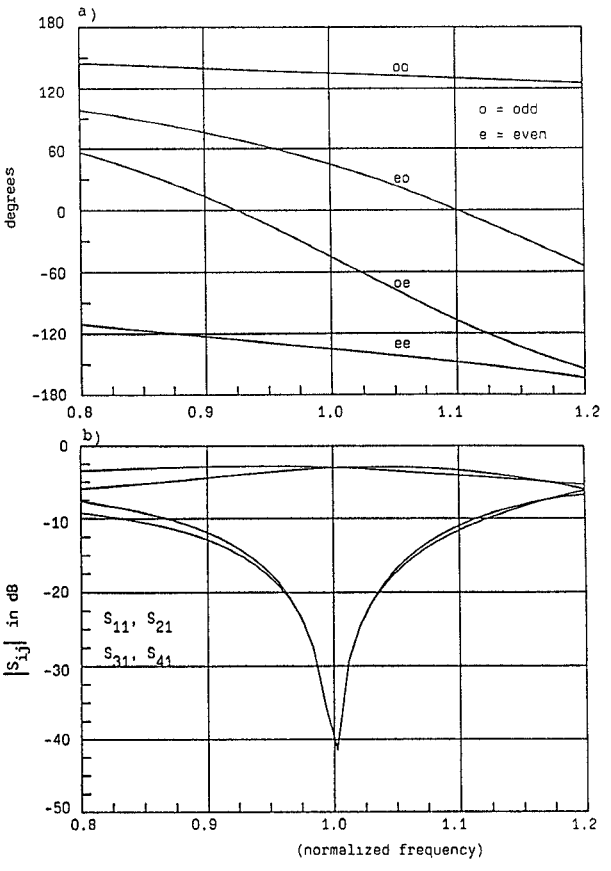

Fig. 5. a) Frequency behaviour of the eigenvalues of a coupler pictured in Fig. 2. All characteristic impedances are set to 70.7Ω. The calculations yield an optimum solution of θ_1 = 26.5°, θ_2 = 35.3°, θ_3 = 56.3° and θ_4 = 35.3° electrical length.
b) Associated S-Parameters

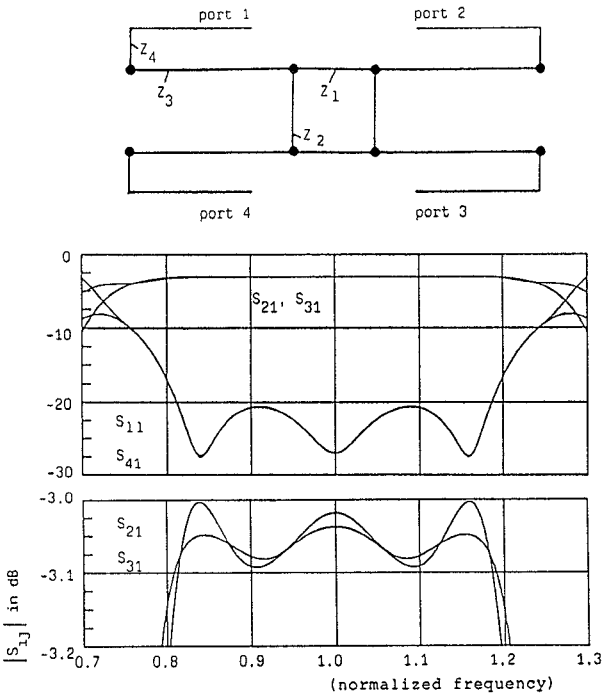

Fig. 6. Theoretical results of a broadbanded coupler pictured in Fig. 1. The characteristic impedances are Z_1 = 38.62Ω, Z_2 = 54.57Ω, Z_3 = 85.5Ω and Z_4 = 34.43Ω. The lengths of the ring branches are a quarter wavelength, the lengths of the serial branches are half-a-wavelength at the center frequency.

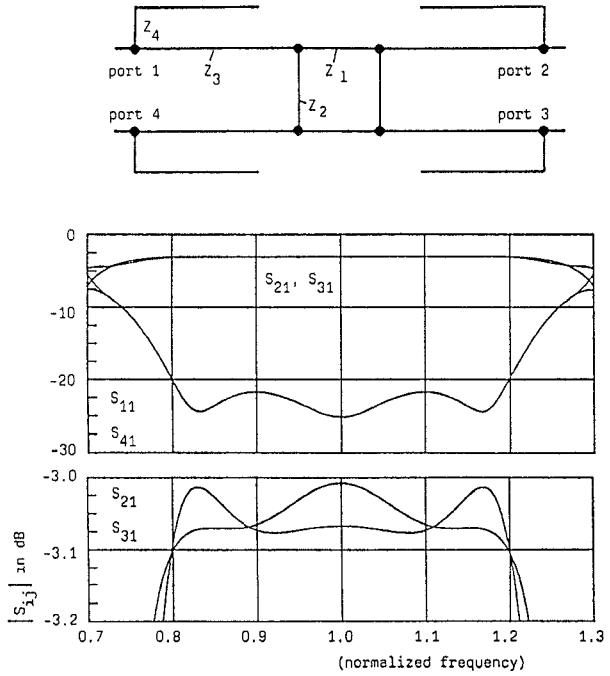

Fig. 7: Theoretical results of a broadbanded coupler pictured in Fig. 1. The characteristic impedances are Z_1 = 39.5Ω, Z_2 = 55.9Ω, Z_3 = 92.7Ω and Z_4 = 67Ω. The lengths of the ring branches are a quarter wavelength, the lengths of the serial branches and of the open stub are half-a-wavelength respectively at the center frequency.

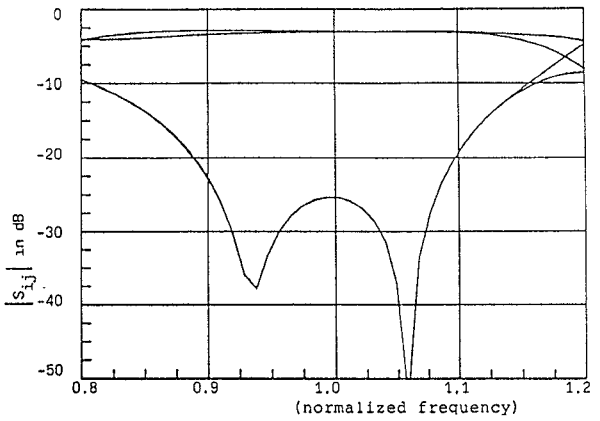

Fig. 8. Theoretical results of the coupler given in Fig. 5, broadbanded with single half-wavelength sections in series to the ports. The characteristic impedances of the additional sections are 95Ω.

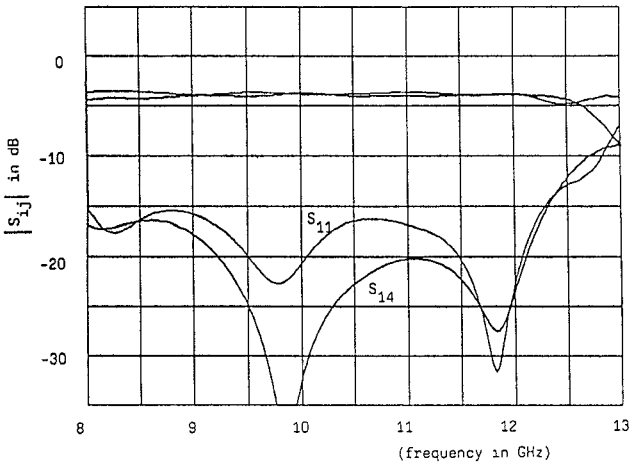

Fig. 9. Measured coupler performance of the coupler described in Fig. 6.

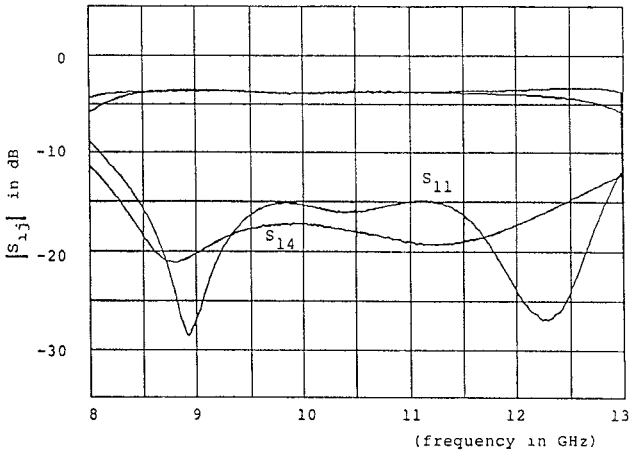

Fig. 10. Measured coupler performance of the coupler described in Fig. 7.